Development of surface phases in $Ba(Zn_{1/3}Nb_{2/3})O_3 - Ba(Ga_{1/2}Ta_{1/2})O_3$ microwave dielectric ceramics.

*H. Hughes, *F.Azough, *R.Freer and +D. Iddles

*Manchester Materials Science Centre, UMIST and University of Manchester, Manchester, M1 7HS, UK

+Filtronic Comtek, Ceramics Division, Enterprise Drive, Station Road, Four Ashes, Wolverhampton WV10 7DB, UK

Abstract:

Ceramics in the system $Ba(Zn_{1/3}Nb_{2/3})O_3 - Ba(Ga_{1/2}Ta_{1/2})O_3$ (BZN -BGT) were prepared by the mixed oxide route. Powders were calcined at 1200`C for 4 hours and sintered at temperatures in the range 1300-1450 ^oC. Products were characterised by SEM, XRD and WDS techniques. Dielectric properties were measured at 3GHz. The end member BZN exhibits ε_r =37 and Qxf = 90,000.

During processing of the ceramics two secondary phases developed on the surfaces of the sintered ceramics as a result of Zn evaporation: $Ba_8Zn_1Ta_6O_{24}$ (816) and $Ba_4Nb_5O_{15}$ (BN). On the basis of this analysis, ceramics having the compositions of the two secondary phases were prepared independently by the mixed oxide route. Both ceramics have a hexagonal structure; the 816 phase has space group of P63cm.

Keywords: perovskites, niobates, secondary phase, dielectric properties

1.Introduction:

Recent developments in wireless communication technology have increased the demand for low cost microwave components. Commercial microwave ceramics need to have specific selective parameters, which are a high unloaded Q value (Q_u > 20000 @ 2GHz), high dielectric constant (ε_r > 30) and temperature coefficient of resonant frequency tuneable through zero. Ba $(Zn_{1/3}Ta_{2/3})O_3$ is an important microwave dielectric, but attempts are being made to develop Nb_2O_5 – based analogues due to the high cost of Ta_2O_5.

The influence of secondary, surface phases on the mechanical and dielectric properties of microwave dielectrics has been discussed by many authors [1,2,3,4,6, 8]. Desu and O`Bryan [4] who first found the presence of the secondary surface phase on sintered BZT ceramics established the connection between the Zn volatilisation, the presence of surface secondary phase and control of dielectric properties.

Later Sumita et al [8] found the presence of the hexagonal $Ba_5Nb_4O_{15}$ phase in $Ba(Mg,Co,Nb)O_3$ based dielectrics and suggested that presence of this impurity phase has a negative effect on dielectric properties. Subsequently Tolmer and Desgardin [3] found a phase believed to be $Ba_8Zn_1Ta_6O_{24}$ in BZT ceramics, but detailed experimental work showed the phase to be $BaTa_2O_6$. The presence of the $BaTa_2O_6$ secondary surface phase was discussed by Webb et al [6] who related the presence of this phase to the high Q value in BZT materials.

In this study ceramics of BZN doped with Ba $(Ga_{1/2}Ta_{1/2})O_3$ (BGT) were prepared by mixed oxide route. The role of secondary phases was investigated.

2. Experimental:

2.1 Ceramic processing

BZN-xBGT (x = 0 - 0.2) and BZCN - 0.1 BGT ceramics were prepared by the mixed oxide route. Standard electronic grade raw materials of purity >99.5% (with a mean particle diameter (d_{50}) ~1-3μm) were batched in lots of 100-200g for the various formulations. The powders were mixed in polypropylene bottles with 200g of ZrO_2 milling media and 100 ml of deionized water for 16 hours. Subsequently they were dried at 80°C, sieved and calcined at 1200 °C for 4 hours. The powders were then re-milled for 8 hours in deionized water containing 2wt% of PEG (MW 20 000) added as binder. After final drying and sieving the powders were pressed into discs of 20mm diameter and sintered at temperatures in the range 1300-1450 °C for 2-16 hours. All samples were sintered in high purity alumina crucibles. All ceramics had > 97% theoretical density as determined by Archimedes water immersion technique.

2.2 Structural and microstructural characterization

Scanning electron microscopy was performed on Philips XL30 FEG-SEM, operating at 8-20 kV. Secondary and backscattered images were recorded. Wavelength dispersive spectroscopy (WDS) was performed on Cameca Electron probe microscope (model SX100), operating at of 15 kV, to yield chemical analyses.

For SEM and WDS analysis the samples were polished with diamond paste (6μm and 1 μm) and with colloidal silica (OPS), and then carbon coated.

Conventional X-ray diffraction analysis was performed on an APD Philips PW3710 with diffractometer operating at 50kV and 40mA. Scans were conducted with Cu K_α radiation with wavelength of 1.54056 Å in the range of 15^o – 35^o with a step size of 0.05^o. The measurements were performed on the surface of the sintered pellets and on sectioned polished samples.

3.Results and Discussion:

3.1 Microstructures

Fig. 1 is a scanning electron micrograph of a BZN sample. The image shows an equiaxed grain structure with grain sizes 5-10μm. There is no visible presence of any secondary phase in the matrix. However, Fig.2 (region near the edge of the BZN sample in Fig.1) shows extensive secondary phases. The chemistry of the second phase was studied by WDS. The thickness of the secondary surface phases in the BZN samples is around 25μm. It is believed that these secondary surface phases develop because of zinc volatilisation.

Fig.3 shows the presence of a secondary surface phases in a BZN ceramic doped with 20% BGT (denoted as BG20). For this composition, the thickness of the secondary surface phase region is about 50μm, i.e. double the thickness in the end member of the BZN composition. An increasing amount of secondary surface phase was observed in the BZN-BGT compositions prepared with higher amounts of BGT.

3.2 Chemical Analysis

WDS analysis of the secondary surface phases showed the presence of two different secondary surface phases. At the outer edge of all samples the $Ba_5Nb_4O_{15}$ phase was found, i.e. all the Zn had evaporated. The thickness of this phase varies with compositions, but for BZN the thickness was around 15μm. The remaining 10μm of secondary surface phase was the $Ba_8ZnNb_6O_{24}$ phase. The presence of the 816 secondary surface phase is consistent with the findings of Davies et al [1] and Bieringer et al [2].

3.3 Phase Analysis

Fig. 4 shows an X ray diffraction spectrum of the matrix of the end member BZN. This spectrum confirms the perovskite structure without any evidence of a secondary phase.

Fig.5 is an X- ray diffraction spectrum for the surface of a sintered BZN specimen. This spectrum shows the presence of secondary phases. It was confirmed that both $Ba_8ZnNb_6O_{24}$ and $Ba_5Nb_4O_{15}$ were present with the BZN matrix. For comparisons purposes samples of the two secondary phases $Ba_5Nb_4O_{15}$ and $Ba_8ZnNb_6O_{24}$ were prepared and analysed. Fig.6 shows XRD spectra for these two phases; they both exhibit the hexagonal structure [1,2,5]; the 816 phase has the space group P63cm

4.Conclusions:

Two secondary phases $Ba_5Nb_4O_{15}$ and $Ba_8ZnNb_6O_{24}$ were found on the surface of sintered BZN-BGT ceramics. The formation of these phases is due to Zn volatilisation. The thickness of the secondary surface phases increases with an increasing amount of BGT in the starting mixture. Both secondary phases exhibit a hexagonal structure.

5. References:

1. Davies, P.K.,Borisevich, A.,Thirumal, M., Communicating with wireless perovskites: cation order and zinc volatilisation, J.Eur.Cer.Soc., 2003, **23,** 2461-2466

2. Bieringer, M., Moussa, S. M., Noailles, L. D., Burrows, A., Kiely, C. J., Rosseinsky, M. J., and Ibberson, R. M., Cation Ordering, Domain Growth, and Zinc Loss in the Microwave Dielectric Oxide $Ba_3ZnTa_2O_{9-\delta}$**,** Chem. Mater., 2003, **15** [2], 586 - 597

3. Tolmer, V., Desgardin, G., Low-Temperature Sintering and Influence of the Process on the Dielectric Properties of Ba(Zn $_{1/3}$ Ta $_{2/3}$)O_3, J.Am. Cer. Soc., (1997), **80** [8], 1981-1991

4. Desu, S.B., O`Bryan, H.M., Microwave loss quality of $BaZn_{1/3}Ta_{2/3}O_3$, J.Am.Ceram.Soc., 1985, **68** [10], 546-551

5. Abakumov, A.M., Van Tendeloo, G.,Scheglov,A.A.,Shpanchenko, R.V., Antipov,E.V.,The crystal structure of $Ba_8Ta_6NiO_{24}$: Cation ordering in hexagonal perovskites, J. Sol. St. Chem., 1996, **125**, 102-107

6. Webb, S.J., Scott, R.I., Cannell, D.S., Iddles, D.M., Alford, N.McN.,Raman spectroscopic study of $Ba(Zn_{1/3}Nb_{2/3})O_3$, J.Am.Cer.Soc., 2002, **85** [7], 1753-1756

7. Kim,D.W., Kwon, D.K., Hong, K.S., Kim, D.J., Atmospheric dependence on dielectric loss of $16Ba_5Nb_4O_{15}{\cdot}56BaNb_2O_6$ Ceramics, J.Am.Ceram.Soc., 2003, **86** [5], 795-799

8. Sumita, S., Kobayashi, M.,Suzuki, K.,Kawamura, K., Miura,T.,Microstrucure and microwave characteristics of $Ba\{(Mg,Co)_{1/3}Nb_{2/3}\}$ – based dielectrics, Jpn.J.Appl.Phys., 1991, 99 [8], 649-653

Figures:

Fig.1. SEM backscattered image of BZN specimen

Fig.2. SEM image of secondary surface phase in BZN specimen.

Fig.3. SEM image of surface secondary phase for BG20 composition

Fig.4. X-ray diffraction spectrum for the matrix of BZN sample.

Fig.5. X-ray diffraction spectrum for the sintered surface of BZN sample. The peaks * correspond to $Ba_5Nb_4O_{15}$; the peaks ** correspond to $Ba_8Nb_6ZnO_{24}$.

Fig.6. X-ray diffraction spectra for specimens of $Ba_8Zn_1Nb_6O_{24}$ and $Ba_5Nb_5O_{15}$.

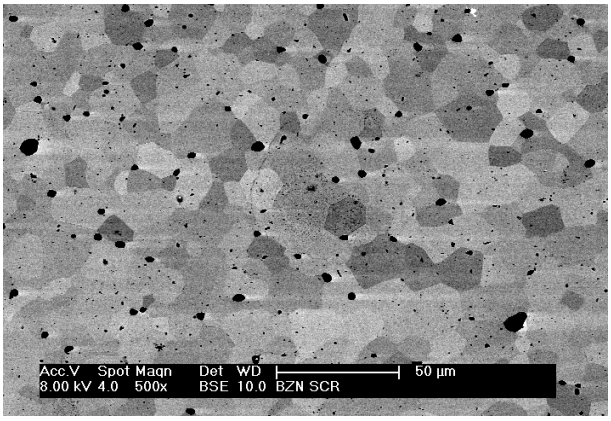

Fig.1 SEM backscattered image of BZN specimen

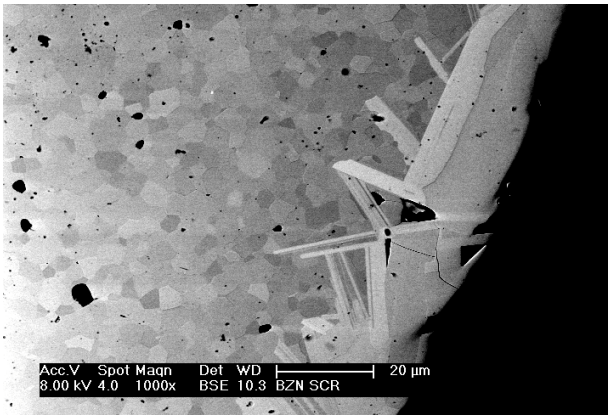

Fig.2 SEM image of secondary surface phase in BZN specimen.

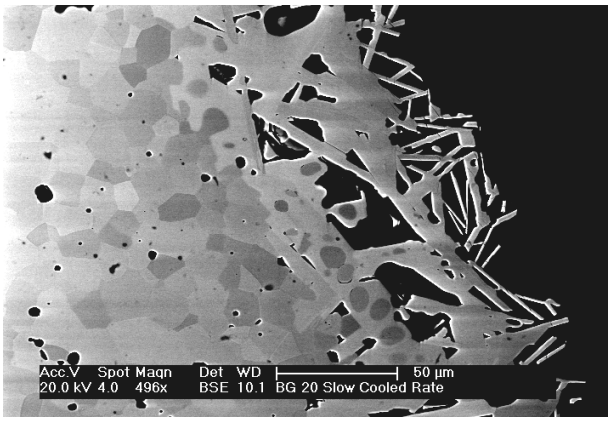

Fig.3 SEM image of surface secondary phase for BG20 composition

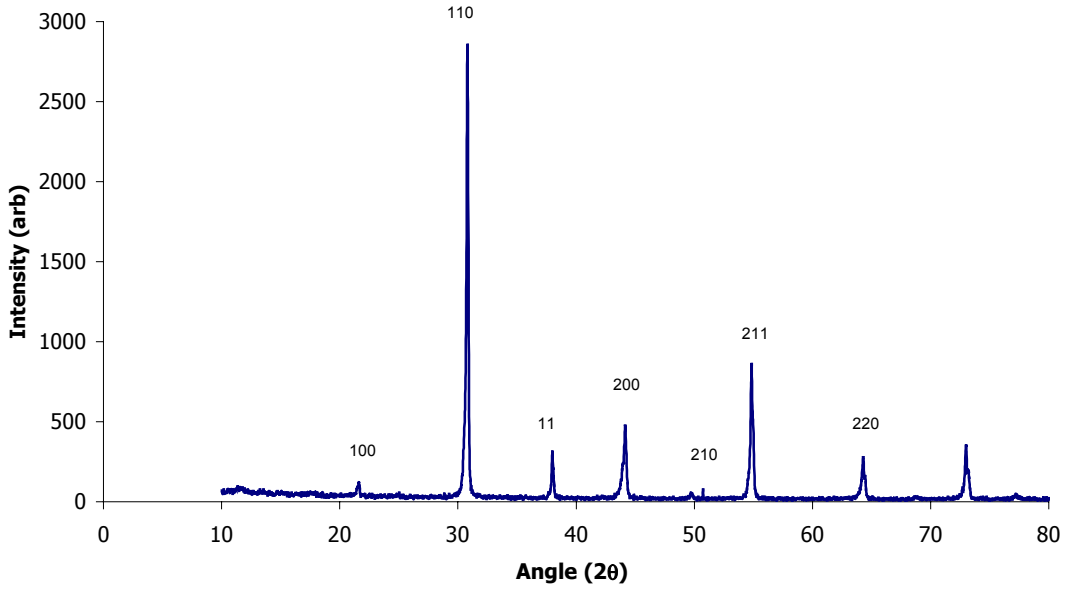

Fig.4 X-ray diffraction pattern for the matrix BZN sample.

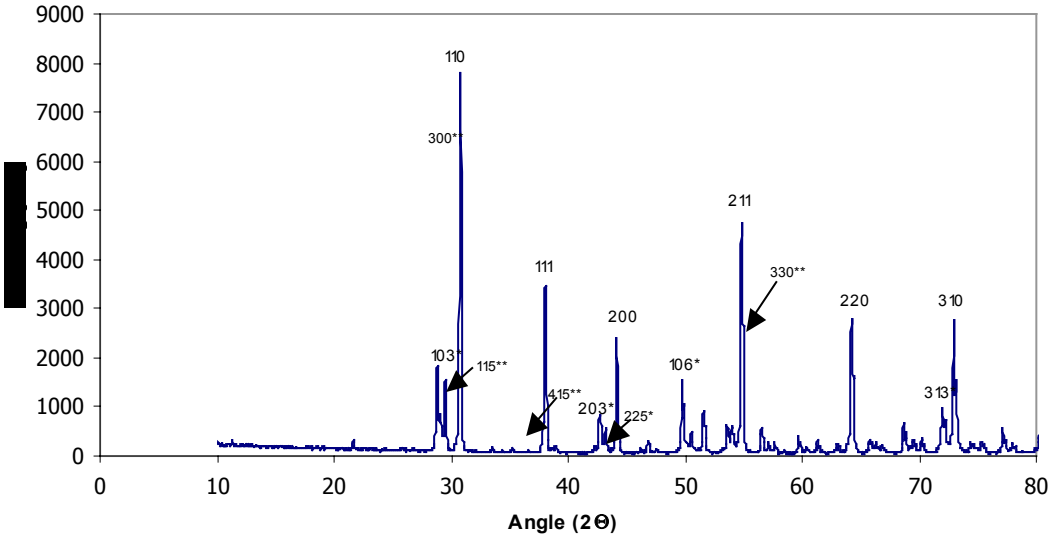

Fig.5 X-ray diffraction pattern for the sintered surface of BZN sample. The peaks * correspond to $Ba_5Nb_4O_{15}$, peaks ** correspond to $Ba_8Nb_6ZnO_{24}$.

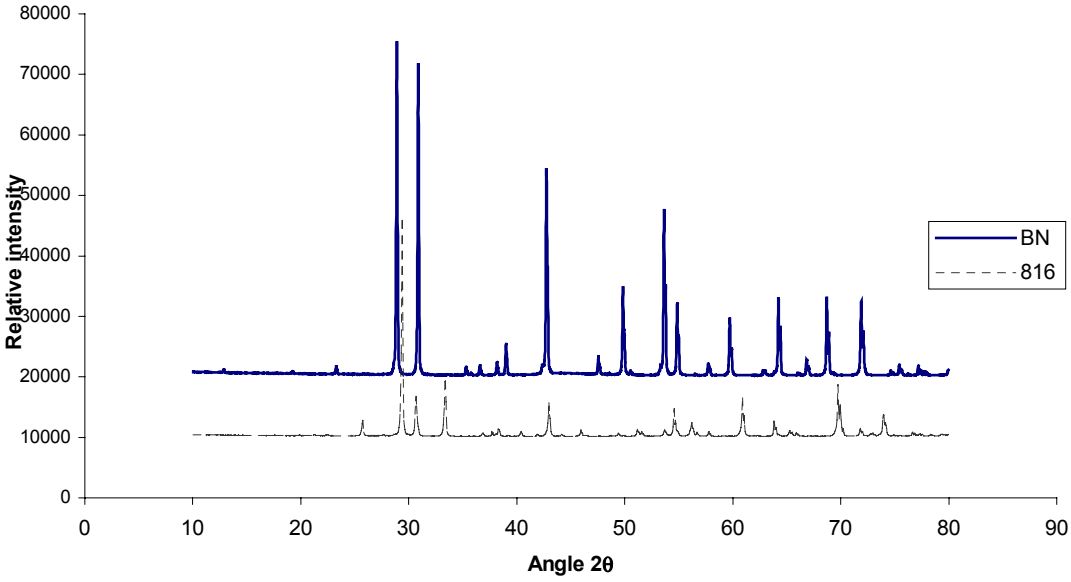

Fig.6 X-ray diffraction spectrum for $Ba_8Zn_1Nb_6O_{24}$ and $Ba_5Nb_5O_{15}$ specimens.